

Article

Online Optimization of Vehicle-to-Grid Scheduling to Mitigate Battery Aging

Qingguang Zhang ^{1,2}, Mubasher Ikram ² and Kun Xu ^{2,*}¹ Electronic and Information Engineering, Southern University of Science and Technology, Shenzhen 518055, China² Shenzhen Institute of Advanced Technology, Chinese Academy of Sciences, Shenzhen 518055, China

* Correspondence: kun.xu@siat.ac.cn

Abstract: The penetration of electric vehicles (EVs) in vehicle-to-grid (V2G) interaction can effectively assist the grid in achieving frequency regulation and peak load balancing. However, the customer perceives that participating in V2G services would result in the additional cycling of the battery and the accelerated aging of the EVs' power battery, which has become a major obstacle to the widespread adoption of V2G services. Most existing methods require long-term cycling data and battery parameters to quantify battery aging, which is not suitable for the V2G scenario with large-scale and short-time intervals. Consequently, the real-time and accurate quantification of battery aging for optimization remains a challenge. This study proposes a charging scheduling method for EVs that can accurately and online quantify battery aging. Firstly, V2G scheduling is formulated as an optimization problem by defining an online sliding window to collect real-time vehicle information on the grid, enabling online optimization. Secondly, battery aging is more accurately quantified by proposing a novel amplitude-based rain-flow cycle counting (MRCC) method, which utilizes the charging information of the battery within a shorter time period. Lastly, an intelligent optimization algorithm is employed to optimize the charging and discharging power of EVs, aiming to minimize grid fluctuations and battery aging. The proposed method is validated using a V2G scenario with 50 EVs with randomly generated behaviors, and the results demonstrate that the proposed online scheduling method not only reduces the EFCC of the battery by 8.4%, but also achieves results close to global optimization.



Citation: Zhang, Q.; Ikram, M.; Xu, K. Online Optimization of Vehicle-to-Grid Scheduling to Mitigate Battery Aging. *Energies* **2024**, *17*, 1681. <https://doi.org/10.3390/en17071681>

Academic Editors: Muhammad Aziz, Minhan Yoon and Don Hur

Received: 27 February 2024

Revised: 22 March 2024

Accepted: 31 March 2024

Published: 1 April 2024



Copyright: © 2024 by the authors. Licensee MDPI, Basel, Switzerland. This article is an open access article distributed under the terms and conditions of the Creative Commons Attribution (CC BY) license (<https://creativecommons.org/licenses/by/4.0/>).

Keywords: smart scheduling; electric vehicle; vehicle-to-grid; battery aging

1. Introduction

From the perspective of the global development trend of the new energy vehicle industry, the large-scale deployment of electric vehicles (EVs) utilizing renewable energy can effectively reduce carbon emissions [1]. In this context, it has ushered in a climax of the industrialization of environmentally friendly and energy-saving vehicles, with new energy vehicles as the main focus. The large-scale integration of EVs will bring significant changes to the overall architecture of the power system. As EVs spend a significant amount of time in parking and charging states [2], it provides a possibility for EVs to participate in grid regulation [3]. EVs' batteries not only provide energy to the onboard powertrains but also serve as an energy storage resource (ESS) to supply energy to the grid. Therefore, the vehicle-to-grid (V2G) interaction between EVs and the grid has attracted much interest from academia and industry.

However, achieving deep integration between the power grid and EVs is still challenging. There have been many studies to promote V2G technology in the recent decade [4,5]. In [6], the authors integrated EVs into the smart grid using a multi-agent reinforcement learning (MARL) approach to optimize peak load management and enhance grid stability. In [7], the authors considered the uncertainty of photovoltaic (PV) and wind power generation, and established a two-stage model to reduce the cost of network operation and

pollution emission. In [8], the authors adopted exact and heuristic approaches to solve EV scheduling and optimal charging problems. In [9], the authors focus on optimizing coordinated schedules for recharging electric buses to enhance charging efficiency and operational cost-effectiveness. In [10], the authors design a robust charging positioning system for electric buses to maintain operational continuity in the event of a charging station failure. The proposed model optimizes the charging plan and considers the mirroring behavior between the primary and standby routes to enhance system resilience in a dynamic environment. The coordinated scheduling of electric vehicle charging involves optimizing the timing and location of charging stations to efficiently meet the charging needs of EVs. The methods presented in [11] aim to minimize waiting times, reduce energy costs and enhance the overall user experience during the charging process. In [12], the authors solve the electric vehicle routing problem with time windows and charging stations. These studies show that V2G enables the bidirectional interaction between the power grid and EVs, which can be utilized to provide power balancing [13,14], reducing grid operation costs [15] and bringing significant benefits to users and the grid [16]. However, the frequent charging and discharging behaviors of EVs in V2G interactions can lead to increased battery cycling, resulting in battery aging [17], which is a major concern for user engagement in V2G.

The aforementioned studies overlook the impact of battery aging on V2G scheduling, which directly affects user participation willingness. Scheduling the charging and discharging behaviors for EVs represents a viable approach to mitigate battery aging among EVs engaged in V2G operations. Some literature investigates the impact of V2G services on the lifespan of onboard lithium batteries through real-life experiments. In [18], the authors conducted V2G experiments on lithium iron phosphate ($LiFePO_4$, LFP) batteries. Tests were performed on batteries with different discharge depths, and it was found that the impact of energy throughput on battery aging was higher than that of cycling depth, regardless of whether V2G services were involved. Therefore, due to the higher energy throughput provided by V2G services, higher degradation was observed. On the other hand, the authors [19] tested nickel cobalt aluminum batteries ($LiNi_xCo_yAl_z$, NCA). The research found that vehicles providing V2G services twice a day had the highest level of capacity degradation, resulting in a battery pack lifespan of less than 5 years.

Some studies suggest that through proper and effective scheduling and regulation, the impact of V2G services on battery aging can be reduced, and even profitability can be created for users. In [20], the authors investigated the influence of frequency regulation on battery aging. After 5 years of usage, the degradation rates of the batteries without V2G services and with V2G services were 7% and 9%, respectively. The authors [21] not only studied the impact of frequency regulation on battery aging but also explored the effects of other factors such as electricity price, charger power, average State of Charge (SoC), and grid frequency characteristics on battery aging and profitability. The simulated scenarios were similar to those in the literature [20]. The results indicated that simulating with a lower average SoC could reduce the battery aging rate, and extend battery lifespan, and if electricity is purchased at industrial prices, V2G services could generate profits for customers.

Existing battery aging models mainly include electrochemical models [22], equivalent circuit models [23], and empirical models [24]. The models mentioned above require either a large number of accurate chemical parameters or extensive data fitting. In V2G scheduling, we can only access limited charging information. Moreover, the charging and discharging power of the battery exhibit continuous variability. Consequently, the above-mentioned battery models are unsuitable for effective implementation in V2G scheduling. In [25], the authors incorporated battery aging as an optimization constraint, utilizing V2G technology to enhance the security and economic feasibility of microgrid systems, thereby reducing operational costs and increasing the absorption of renewable energy. In [26], the authors considered battery aging in the V2G scheduling process, using battery aging as the objective function and employing the rain-flow counting (RCC) method to quantify battery aging, thereby actively mitigating battery aging and alleviating grid fluctuations.

Nevertheless, the conventional RCC method may not accurately characterize the aging behaviors of the battery, particularly within the dynamically varying charge and discharge processes of V2G. This inadequacy may result in substantial errors in the quantification of the battery aging process.

To effectively mitigate battery aging in V2G services and enhance user participation in V2G services, this study proposes a novel charge and discharge scheduling optimization method for multiple EVs in V2G scenarios. The main contributions are as follows: (1) proposing a new RCC method to accurately quantify battery aging behaviors in V2G services; (2) leveraging an online V2G scheduling paradigm utilizing a time-varying sliding window to collect real-time vehicle information for online scheduling optimization and (3) establishing an online V2G scheduling model to minimize grid load fluctuations and equivalent cycle counts of the batteries.

The remaining sections are arranged as follows. Section 2 presents the structure of the V2G scheduling system, as well as the energy and information flow during the scheduling process. The V2G scheduling modeling method and the proposed battery aging quantification method used in this study are described in Section 3. Results and discussions are provided in Section 4, followed by concluding remarks in Section 5.

2. V2G Scheduling System Architecture

The architecture of the V2G scheduling system discussed in this paper is shown in Figure 1. The system is divided into three parts: the load side composed of client side and grid side, the online scheduling system guiding vehicle charging, and the optimization system considering battery aging and grid fluctuations. Through the collaboration of these three parts, the optimal V2G charging scheduling is achieved.

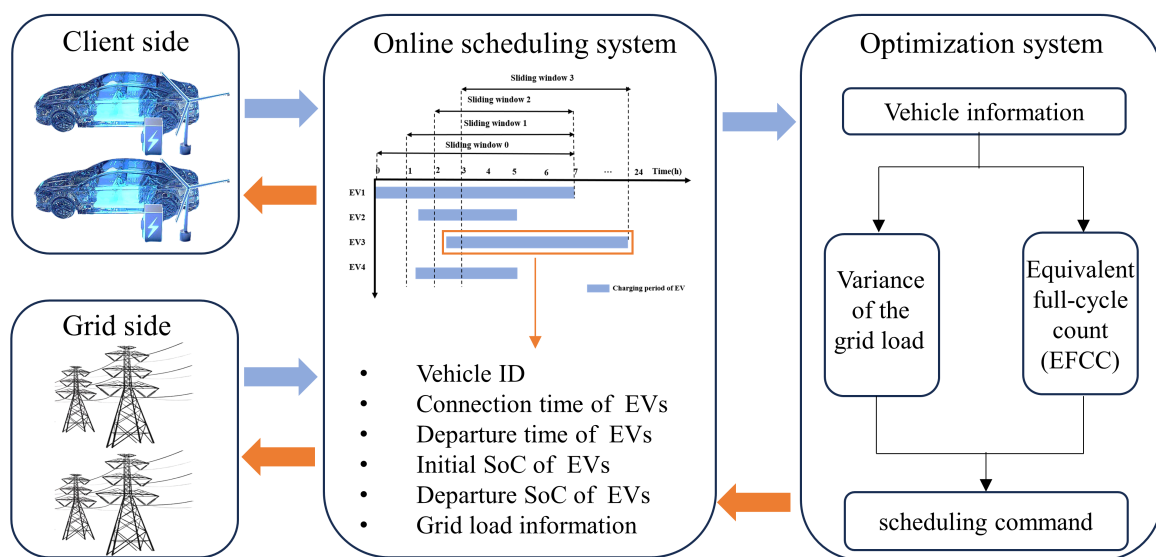


Figure 1. V2G scheduling system architecture.

There are two categories of information collected on the client side: one is user-defined information and the other is information retrieved by the system based on the current status. When customers arrive at the parking lot, they need to input information about their EVs, including the departure time of EVs, the Departure SoC of EVs, and the rated capacity of the battery. Subsequently, the client-side retrieves the information based on the current status, which includes the vehicle ID, the Connection time of EVs, and the Initial SoC of EVs. The grid side collects information on electricity consumption in residential areas and these serve as the base load for the grid. All the mentioned information is then transmitted to the online scheduling system.

The online scheduling system is used to receive base load and EVs' charging demand data transmitted from the load side, using Information and Communications Technology (ICT) [27]. The online sliding window algorithm has been widely applied in various fields [28]. This method allows decision-makers to make use of data that are revealed as time progresses [29]. In [30], the sliding window algorithm is incorporated into the methodology to address the charging scheduling problem for electric buses while optimizing the utilization of renewable energy. In this paper, we utilize the online sliding window to record and update information on EVs connected to the grid and base load, subsequently sending them to the optimization system. Section 3.2 will provide a detailed introduction to the definition of online sliding windows.

The V2G scheduling is mathematically modeled as an optimization problem in the optimization system. The objective is to minimize both grid load fluctuation and battery degradation. The grid load fluctuation is quantified by the standard deviation, while battery degradation is measured by equivalent full-cycle count (EFCC).

$$EFCC = \frac{N \times A}{Q} \quad (1)$$

where N denotes the number of cycles of the battery, A is its corresponding amplitude, and Q is the capacity of the battery. Intelligent optimization algorithms use collected user demands and grid load status to develop V2G charge/discharge control strategies for each connected EV. Control instructions are sent to the online scheduling system to guide the orderly charging of EVs.

3. Methodology

3.1. Magnitude-Based Rain-Flow Cycle Counting

The degradation mechanism of batteries has been well explained in past research. Existing methods for battery aging include electrochemical models [22], equivalent circuit models [23], and empirical models [24], all of which require long-term (days or months) charge/discharge data to quantify battery aging. However, in V2G scheduling, the time frame is often less than a day or even several hours, rendering the above methods unsuitable for V2G scheduling. RCC is an intuitive and graphical method for fatigue analysis of materials. By counting and statistically analyzing strain-time history data, it is widely used in engineering practice for fatigue life assessment and material design [31].

RCC has been applied in V2G scheduling to quantify battery aging. The RCC algorithm is mainly implemented through the following three steps, as shown in Figure 2. First, the SoC curve of the battery is analyzed to remove the plateau sections and retain the alternating peaks and valleys. This accurately identifies the charge/discharge cycles of the battery. Next, the obtained curve is traversed, and the four-point method is used to count the total number of cycles. By identifying the peaks and valleys in the load history and calculating the amplitude and mean value between adjacent peaks and valleys, the complete charge/discharge cycles can be determined. Finally, the remaining portion of the curve is divided into corresponding half-cycles, and the count is recorded. This provides a more comprehensive cycle counting result. Through Figure 2f, it can be observed that although they are all one full-cycle or half-cycle, there are still certain differences. The height of each triangle represents the amplitude corresponding to that cycle. Therefore, only counting the number of cycles of the battery while ignoring the amplitude can lead to significant errors.

In [26], RCC quantifies the aging of the battery in V2G scheduling by converting the battery's SoC curve into the number of full-cycles N^c and half-cycles N^{h-c} . The SoC of batteries under two different operating conditions is shown in Figure 3. After applying the RCC processing to the two sets of data within the red box, the full-cycle count N^c is 1, and the half-cycle count N^{h-c} is 2. However, in reality, the degree of degradation of the battery under these two operating conditions is different. In V2G scheduling, as the number of EVs increases, the frequency of this phenomenon also increases. Simply counting N^c and N^{h-c} results in increased errors for the client. Therefore, this paper proposes the RCC

considering the amplitude (MRCC). MRCC multiplies the amplitude by its corresponding cycle number to convert it into the EFCC of the battery, which can more accurately quantify the battery aging phenomenon in the optimization system.

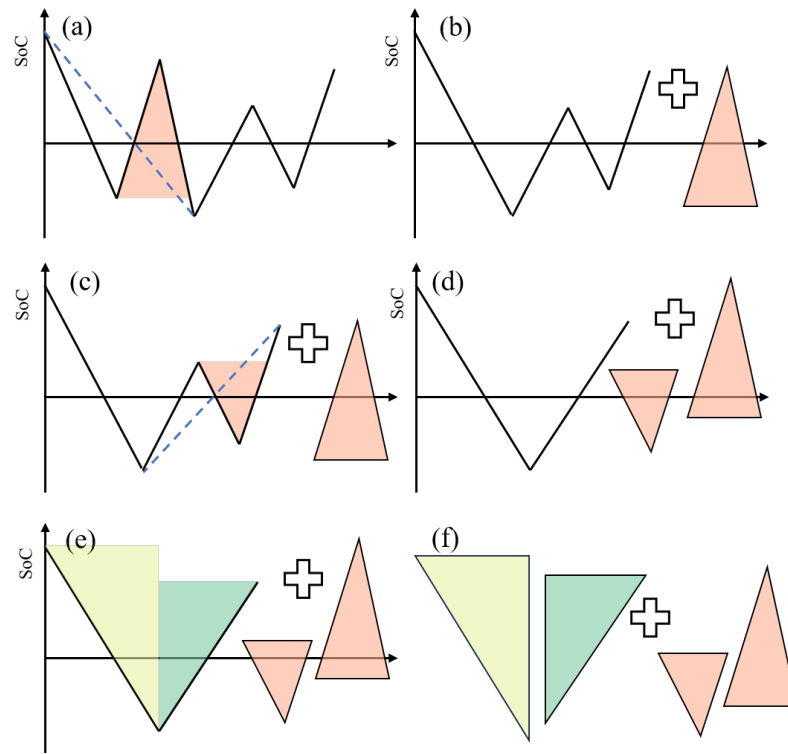


Figure 2. The process of extracting battery cycles in the rain-flow cycle counting algorithm. (a) Raw data. (b–d) The four-point method of extracting the full-cycle count. (e) The extracted half-cycle count. (f) The extracted battery cycles.

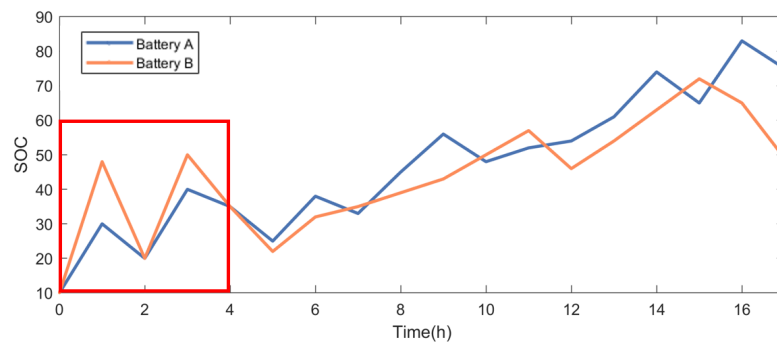


Figure 3. Battery State of Charge (SoC) curve.

3.2. Online Sliding Window

When participating in V2G services, the system records the current time point t and retrieves EVs' information based on the actual situation, including the EVs number i , connection time of EVs T_i^S , initial SoC of EVs $SoC_{i,t}$, and current status of EVs $stat_{i,t}$. Subsequently, the system requires the client to provide information on EVs, including the estimated departure time T_i^E , desired SoC at departure SoC_i^{set} , and the rated capacity of battery Q_i . $stat_{i,t}$ represents the status of EV i at time t . If the value of $stat_{i,t}$ is 1, it indicates that EV i is available for dispatch at time t . If the value of $stat_{i,t}$ is 0, it means that EV i is not connected to the grid or not available for dispatch at time t . If the value of $stat_{i,t}$ is 2, it means that EV i has completed the scheduling task at time t .

The sliding window is used to collect EVs' information and perform real-time updates. EVs' information collected by the sliding window at time t is stored in E_t . If EV i satisfies $T_i^S \leq t$ and $T_i^E > t$, and $stat_{i,t} = 1$, then the information of this EV will be recorded in the EV collection E_t . As time progresses, the data in E_t keep updating. This also leads to the continuous change in the length of the sliding window. The starting time of the sliding window, T_{cur}^S is equal to the current time t , and the ending time of the sliding window is defined as $T_{cur}^E = \max\{T_i^E | i \in E_t\}$.

The definition of the sliding window is illustrated in Figure 4. Firstly, the time that four EVs were involved in V2G scheduling was counted and represented by blue bars in the figure. Then, based on the definition mentioned above, we can observe that at $t = 0$, only EV_1 satisfies $T_i^S \leq t$, $T_i^E > t$ and $stat_{i,t} = 1$, thus $E_0 = EV_1$. Therefore, the ending time of sliding window 0 is calculated as $T_{cur}^E = \max\{T_i^E | i \in E_0\} = 7$. Similarly, at $t = 2$, EV_1, EV_2 , and EV_4 satisfy $T_i^S \leq t$, $T_i^E > t$ and $stat_{i,t} = 1$, so $E_2 = \{EV_1, EV_2, EV_4\}$. Thus, the ending time of sliding window 2 is calculated as $T_{cur}^E = \max\{T_i^E | i \in E_2\} = 7$. By applying the same method, the information for sliding windows 0 and 3 can be determined. The sliding window only sends the currently collected information to the optimization system for further optimization.

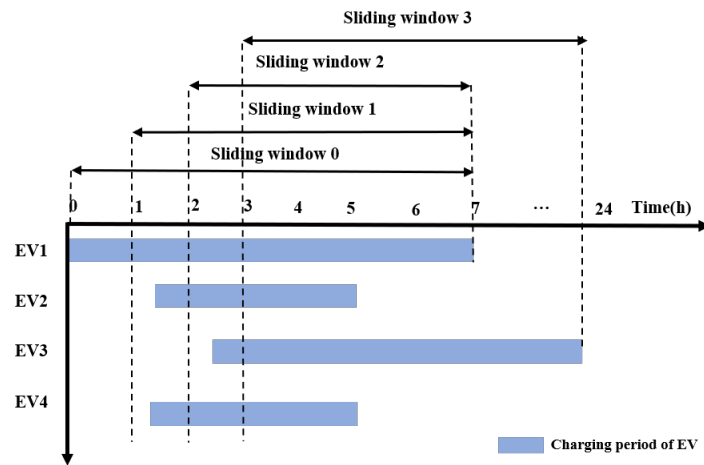


Figure 4. The sliding window for online optimization.

3.3. V2G Scheduling Modeling

In this algorithm, the optimization variables are the charge/discharge power of EVs at each time step. The information about EVs and their availability during the online period denoted as $stat_{i,t}$ is collected using the sliding window defined in this paper. The particle dimension is $(m \times w)$. Where $m = T_{cur}^E - T_{cur}^S$ represents the length of the current sliding window. $w = \text{num}(E_t)$ is the number of EVs in the current sliding window. A matrix of EVs' charge/discharge power P_{ev} is constructed according to Equation (2). Where $P_{ev_w(m)}$ is the charge/discharge power of vehicle w -th at time m .

$$P_{ev} = \begin{bmatrix} P_{ev_1(1)} & P_{ev_1(2)} & P_{ev_1(3)} & \dots & P_{ev_1(m)} \\ P_{ev_2(1)} & P_{ev_2(2)} & P_{ev_2(3)} & \dots & P_{ev_2(m)} \\ \dots & \dots & \dots & \dots & \dots \\ P_{ev_w(1)} & P_{ev_w(2)} & P_{ev_w(3)} & \dots & P_{ev_w(m)} \end{bmatrix} \quad (2)$$

The objective function consists of two terms. Firstly, the grid load variance is used to reflect the fluctuations in the electric grid, aiming to achieve peak load balancing. Secondly, EFCCs based on MRCC are used to quantify battery aging.

According to the historical data from the local grid, the real-time grid variance is expressed as:

$$fitness1 = \min \left\{ \frac{\sum_{t=1}^m [P_{load}(t) + \sum_{i=1}^w P_{ev,i}(t) - P_{AV}]}{m} \right\} \quad (3)$$

where $P_{load}(t)$ is the base load power of the grid in the time slot t , P_{AV} is the average grid load, $P_{ev,i}(t)$ is the power of the i -th vehicle at the time slot t .

During the optimization process, MRCC is employed to calculate the cycle counts of the SoC curves of the battery that can capture the corresponding capacity amplitude. The expression for EFCC is as follows:

$$fitness2 = \min \left\{ \sum_{i=1}^w \left(N_i^c A_i^c + \frac{N_i^{h-c} * A_i^{h-c}}{2} \right) \right\} \quad (4)$$

where N_i^c and N_i^{h-c} are the battery number of cycles and half-cycles of EV_i . A_i^c is the amplitude of N_i^c , and A_i^{h-c} is the amplitude of N_i^{h-c} .

The overall objective function is defined as:

$$fitness = b_1 \cdot fitness1 + b_2 \cdot fitness2 \quad (5)$$

where b_1 and b_2 are weight parameters. The variation in the charge/discharge power of EVs can impact the load variance of the power grid. Similarly, different charge/discharge power levels can also cause changes in the EFCC of the battery. Therefore, it is necessary to allocate the charge/discharge power of EVs in different time periods appropriately to achieve V2G scheduling.

The main constraints from the battery include the SoC, charge/discharge power, and departure SoC of EVs, as shown in (6).

$$St. \begin{cases} SoC_{min} \leq SoC_{i,t} \leq SoC_{max} \\ -P_{i,dis}^{max} \leq P_{i,t} \leq -P_{i,dis}^{min} \\ P_{i,chg}^{min} \leq P_{i,t} \leq P_{i,chg}^{max} \\ SoC_i^E \geq SoC_i^{set} \end{cases} \quad (6)$$

where SoC_{min} and SoC_{max} , respectively, represent the minimum and maximum values allowed for SoC, $SoC_{i,t}$ represents the SoC of the i -th vehicle at time t . $P_{i,dis}^{max}$ and $P_{i,dis}^{min}$, respectively, represent the maximum and minimum allowed discharge power, $P_{i,t}$ represents the power of the i -th vehicle at time t . $P_{i,chg}^{max}$ and $P_{i,chg}^{min}$, respectively, represent the maximum and minimum allowed charging power. SoC_i^E is the SoC of EV i -th when leaving, SoC_i^{set} is the minimum SoC required for EV when leaving.

3.4. Particle Swarm Optimization

The Particle Swarm Optimization (PSO) algorithm possesses global search capabilities, enabling it to find optimal solutions to complex optimization problems. Compared to other optimization algorithms, the PSO algorithm is known for its simplicity, efficiency, and fast computation. Additionally, the PSO algorithm is applicable to solving non-continuous and non-convex optimization problems, such as V2G scheduling. With its ability to handle large-scale problems and high-dimensional spaces, the parallelizability of PSO allows for utilizing multiple processing units, thereby enhancing optimization efficiency and performance. The conventional convex optimization method [32] is not applicable in V2G scheduling due to the typically non-linear or non-quadratic nature of the objective function. Additionally, the introduction of the battery degradation index transforms the optimization objective into a noncontinuous, non-derivable, and non-gradient function,

rendering conventional gradient descent algorithms ineffective [33]. Therefore, the PSO algorithm is employed in this study for solving V2G scheduling strategies.

The flowchart of the PSO algorithm is shown in Figure 5. Firstly, the particles' positions and velocities need to be initialized. Assuming the target problem is n -dimensional, the position of a particle in the n -dimensional solution space is represented as $X_a = X_{a,1}, X_{a,2}, \dots, X_{a,n}$, where a denotes the particle's index in the population, and $X_{a,b}$ represents the position component of the a -th particle in the b -th dimension. The flying velocity of the particle is represented as $V_a = V_{a,1}, V_{a,2}, \dots, V_{a,n}$, where $V_{a,b}$ denotes the velocity component of the a -th particle in the b -th dimension. The particles' positions and velocities are randomly generated within the feasible range.

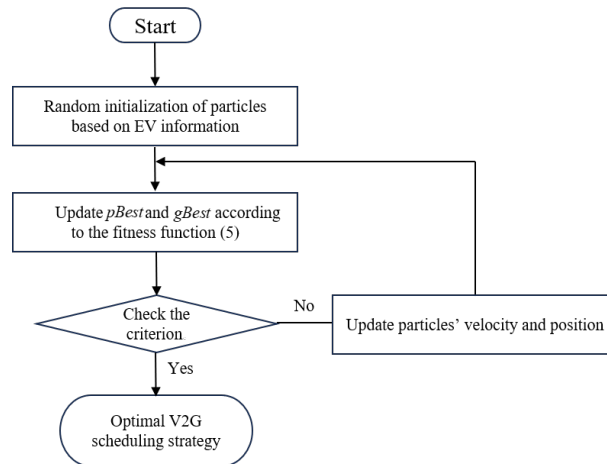


Figure 5. The flowchart of the PSO algorithm.

Next, the fitness of each particle is evaluated based on the objective function, which allows for the calculation of individual best positions and the global best position of the population. For each particle, an evaluation of the fitness value is performed based on the objective function of the optimization problem. The fitness values determine the relative performance of each particle. Based on these values, the best position found by the a -th particle during the search process is recorded and dynamically updated, denoted as $pBest_a$. After all the particles have computed and updated their individual best positions, the global best position, denoted as $gBest$ is determined by comparing the individual best positions among the entire population. The global best position represents the collective experience of the population and guides the particles toward the optimal solution.

After obtaining $gBest$, the convergence criterion is checked to determine if it is satisfied. If the criterion is met, the algorithm outputs the optimal result. Otherwise, the algorithm continues to the next step.

After computing and updating the individual best position and the global best position, each particle needs to update its velocity based on these two values. The velocity update formula for the a -th particle is as follows:

$$V_a(t+1) = wV_a(t) + c_1r_1(pBest_a(t) - X_a(t)) + c_2r_2(gBest(t) - X_a(t)) \quad (7)$$

where w is the inertia weight, representing the degree to which the previous velocity is retained. The inertia weight allows control over the influence of the particle's prior velocity on the current velocity. c_1 and c_2 are the learning factors, also known as acceleration constants, representing the strength of the particle's learning ability towards the individual best position and the global best position, respectively. They can adjust the maximum step size of the particle's flight towards the individual best position and the global best position. r_1 and r_2 are random numbers between 0 and 1, enhancing the randomness of particle flight to ensure search capability. The aforementioned steps are repeated continuously until the convergence criterion is satisfied.

4. Results and Discussions

4.1. Simulation Setup and Dataset

The EVs' travel data in this study are sourced from the 2017 National Household Travel Survey (NHTS) [34]. It provides a daily travel diary for the United States and its major census divisions and supplementary regions. It is the sole national-level statistical data source for individual travel in the United States. This survey series (conducted since 1969) includes demographic data on households, populations, and vehicles, as well as detailed information on daily travel for various transportation modes and destinations.

The probability of private EV users' trips is mainly influenced by their daily habits and routines. To begin with, it is necessary to obtain the distribution of initial departure times. The departure time distribution can be fitted using a normal distribution. The probability density function for the users' daily trip can be expressed as:

$$f_1(x_1) = \begin{cases} \frac{1}{\sqrt{2\pi}\sigma_1} \exp\left(-\frac{(x_1 - \mu_1)^2}{2\sigma_1^2}\right) & 0 \leq x_1 < \mu_1 + 12 \\ \frac{1}{\sqrt{2\pi}\sigma_1} \exp\left(-\frac{(x_1 - \mu_1 - 24)^2}{2\sigma_1^2}\right) & \mu_1 + 12 \leq x_1 < 24 \end{cases} \quad (8)$$

where x_1 represents the departure time of EV users, expected value $\mu_1 = 7.39$, and standard deviation $\sigma_1 = 3.49$. After obtaining users' travel data randomly using the Monte Carlo algorithm, only the data within the time period of 16:00–24:00 and 0:00–8:00 are retained. All charging tasks for EVs need to be completed within this time frame.

Based on the analysis of travel habits and patterns, the final destinations driven by most users are highly random. However, the average daily driving distance is approximately 38 km/d. The daily driving distance of EV users follows a log-normal distribution, with the probability density function given by:

$$f_2(x_2) = \frac{1}{x_2\sigma_2\sqrt{2\pi}} \exp\left(-\frac{(\ln x_2 - \mu_2)^2}{2\sigma_2^2}\right) \quad (9)$$

where x_2 represents the driving distance of EV users, expected value $\mu_2 = 2.92$, and standard deviation $\sigma_2 = 0.93$.

The SoC of vehicle batteries, daily average driving distance, charging patterns, and charging time are statistically analyzed [35]. The remaining SoC of EVs upon return can also be fitted using a normal distribution. The probability density function of the remaining SoC of EVs is as follows:

$$f_3(x_3) = \frac{1}{\sqrt{2\pi}\sigma_3} \exp\left(-\frac{(x_3 - \mu_3)^2}{2\sigma_3^2}\right) \quad (10)$$

where x_3 represents the remaining SoC of the EV upon return, expected value $\mu_3 = 51.3$, and standard deviation $\sigma_3 = 14.7$.

The SoC of vehicle batteries during user travel needs to meet the daily travel requirements. Based on the daily driving distance of each EV and the average energy consumption per kilometer, the daily energy demand can be calculated as follows:

$$SoC_{demand} = \frac{x_2 \times E_{ev}}{Q_{ev}} \quad (11)$$

where E_{ev} represents the average energy consumption per kilometer of the vehicle, and Q_{ev} represents the capacity of the battery. When the vehicle owner selects their desired SoC upon departure, SoC_{demand} can provide guidance, meaning that SoC_i^{set} must be greater than or equal to SoC_{demand} .

In simulation, we use the Monte Carlo algorithm to obtain the expected value of E_{ev} according to Equation (9). We generate the SoC when the EV is connected to the grid based on Equation (10), and use Equation (11) to guide the provision of the total amount

of electricity to be charged for participating in V2G. The dataset generated based on the above formula is shown in Table 1.

Table 1. An example charging segment of the collected datasets.

Vehicle ID	Connection Time	Initial SoC	Departure Time	Departure SoC	Current Status	Capacity of Battery (kW·h)
1	22:58	40%	6:12	56%	0	100
2	16:24	78%	7:20	88%	0	100
...
49	18:38	51%	5:30	66%	0	100
50	17:05	63%	6:18	82%	0	100

The individuals' travel behavior data, including the vehicle ID, EVs' grid-connected time and SoC, departure time and SoC, battery system parameters, etc., are further extracted from the collected data set to simulate the users' V2G behaviors and verify the proposed scheduling method.

The simulation parameters are shown in Table 2. This study focuses on the most active V2G periods (16:00–24:00 and 00:00–08:00). There are several reasons for selecting these two time periods. Firstly, these periods coincide with peak energy demand, which corresponds to the highest electricity consumption. Allowing EVs to discharge power during these periods enables the grid to access additional energy to meet the increased demand. During other time periods, there are typically fewer EVs available for V2G scheduling as most EVs are not at charging stations. Secondly, during the nighttime period (00:00–08:00), electricity demand is generally lower. EVs can utilize this time to charge, helping to balance the grid load and store excess power for use during peak periods. Lastly, these time periods hold the greatest market potential for EVs participating in the V2G market. With a higher rate of charging and discharging activities and increased grid load volatility during these periods, properly scheduling the charge/discharge power of EVs can yield greater V2G market benefits. Scheduling is performed for the online vehicles every 30 min, with a total of 50 EVs participating in V2G.

Table 2. The parameters of the simulation environment.

Parameters	Value
V2G period	16:00–24:00 and 0:00–8:00
Base load sampling interval	30 min
Number of vehicles	50
Maximum and minimum battery SoC	90% & 5%
Maximum battery V2G charging and discharging power	10 kW & 20 kW

The parameter settings for the PSO algorithm used in this study are shown in Table 3 and were determined through multiple experiments to achieve improved performance:

Table 3. The parameters of PSO algorithm.

Parameters	Value
Iteration times	150
Population size	2000
Learning factor	$c1 = 1.49$ and $c2 = 1.49$
weight parameters	$b1 = 1$ and $b2 = 400$
Penalty factor	5000
Inertia weight	0.9

The baseline load curve of the grid and the curve of unscheduled charging of EVs are shown in Figure 6. We can observe that the integration of EVs increases the load fluctuation on the grid and also raises the peak value of grid electricity consumption. This is detrimental to the power grid.

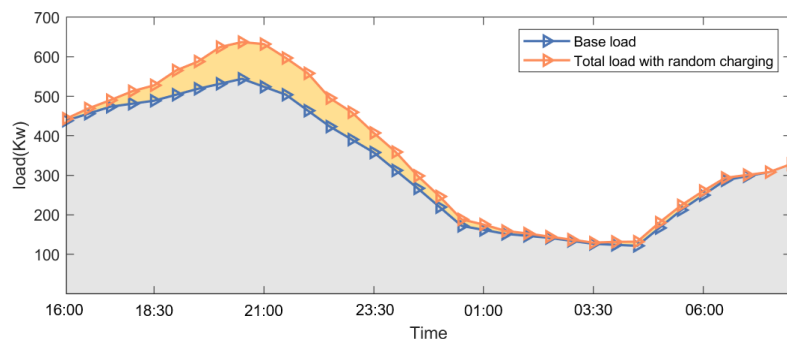


Figure 6. The power system baseload and total load profile when EVs random charging.

4.2. The Results of V2G Scheduling

Global optimization offers advantages such as finding the global optimum solution to a problem, improving the robustness of solutions, applicability to various problem types, and efficiency. It is widely applied across different fields. It can find optimal solutions to complex problems and provides powerful tools and methods for solving practical, complex issues. Global optimization refers to the assumption that we have access to the behavior information of all charging vehicles for a specific day and conduct offline optimization using the PSO algorithm. However, as the EVs' information in V2G scenarios cannot be known in advance, global optimization is not applicable in this context. In this study, an online sliding window approach is used to optimize the problem in real time, collecting EVs and grid parameter information every 30 min. After each optimization, only the charge/discharge power of EVs in the current time period is extracted for V2G scheduling.

We conducted multiple experiments using the same vehicle behavior and simulation parameters. After considering the global particle swarm optimization algorithm with RCC (G-PSO-RCC) for V2G scheduling, it showed better performance in peak shaving, grid fluctuation mitigation, and battery aging compared to uncontrolled charging. It can meet the demands of V2G services and EV owners. The peak load of the grid was measured to be 453.79 kW, with a standard deviation (STD) of 28.42 and EFCC of 35.92. However, this method requires obtaining all EVs and grid information for the day at the beginning of the scheduling, which is not feasible in practical scenarios due to factors such as geographical location, time, and weather. By using the online particle swarm optimization algorithm with RCC (O-PSO-RCC) for scheduling, the peak load of the grid was measured to be 460.97 kW, with an STD of 27.34 and an EFCC of 36.20. Compared to G-PSO-RCC, O-PSO-RCC showed a 1.58% increase in peak load and a 0.78% increase in EFCC, while reducing the STD by 3.8%. O-PSO-RCC not only achieves results similar to G-PSO-RCC but also meets the requirements of practical scheduling scenarios. Therefore, the subsequent research in this paper mainly focuses on the use of online scheduling algorithms.

The V2G scheduling model developed in this study can be viewed as a Pareto problem. The grid load variance and the battery's EFCC are mutually constrained, making it impossible to simultaneously minimize both factors. In the absence of consideration for battery aging, the V2G scheduling tends to prioritize the grid side. Hence, compared to uncontrolled charging, the optimization using G-PSO-RCC lowers the peak grid load to 453.6 kW and reduces the STD to 7.49. However, the EFCC increases to 45.93, indicating excessive battery usage. To address this, RCC is employed to quantify battery aging and incorporate it into the V2G scheduling. Through G-PSO-RCC optimization, the EFCC of the battery is reduced by 21.79%, effectively alleviating battery aging. Although the STD increases to 28.42, this value remains acceptable for the grid side.

The V2G scheduling results based on the RCC algorithm are shown in Figure 7a. During the peak grid time, EVs are scheduled to feed energy back to the grid, ensuring that the peak charging load of EVs no longer overlaps with the peak load of the baseline grid, successfully reducing the peak grid load. However, there is a significant error in the assessment of EVs' batteries aging during this process. In large-scale V2G scheduling scenarios, this could lead to even greater losses for the battery. To further improve the ability to quantify battery aging, this paper proposes an MRCC method, with results shown in Figure 7b. As shown in Table 4 with the proposed method, the V2G scheduling system not only achieves long-term load transfer performance but also suppresses short-term grid load fluctuations. Compared to random charging, the peak load and STD of the load are reduced by 28.35% and 88.99%, respectively. Compared to traditional V2G scheduling methods, the EFCC and STD in this paper's V2G scheduling method are reduced by 8.4% and 28.57%, respectively. This indicates that the method not only suppresses battery degradation phenomena in V2G services but also suppresses short-term grid load fluctuations.

Table 4. The result of different V2G management method.

Scenario	Peak (kW)	STD	EFCC
Base load	544.24	149.06	-
Random charging	637.24	177.47	31.64
V2G & G-PSO	453.60	7.49	45.93
V2G & G-PSO-RCC	453.79	28.42	35.92
V2G & O-PSO-RCC	460.97	27.34	36.20
V2G & O-PSO-MRCC	456.57	19.53	33.16
V2G & O-GWO-RCC	510.52	60.90	31.11
V2G & O-GWO-MRCC	506.20	55.52	29.92

To validate the robustness of the V2G modeling proposed in this paper, we employed the grey wolf optimization (GWO) algorithm for V2G scheduling optimization. After optimization with GWO, similar results were obtained compared to PSO. When comparing the GWO-MRCC algorithm with the GWO-RCC algorithm, the EFCC and STD decreased by 3.82% and 8.83%, respectively.

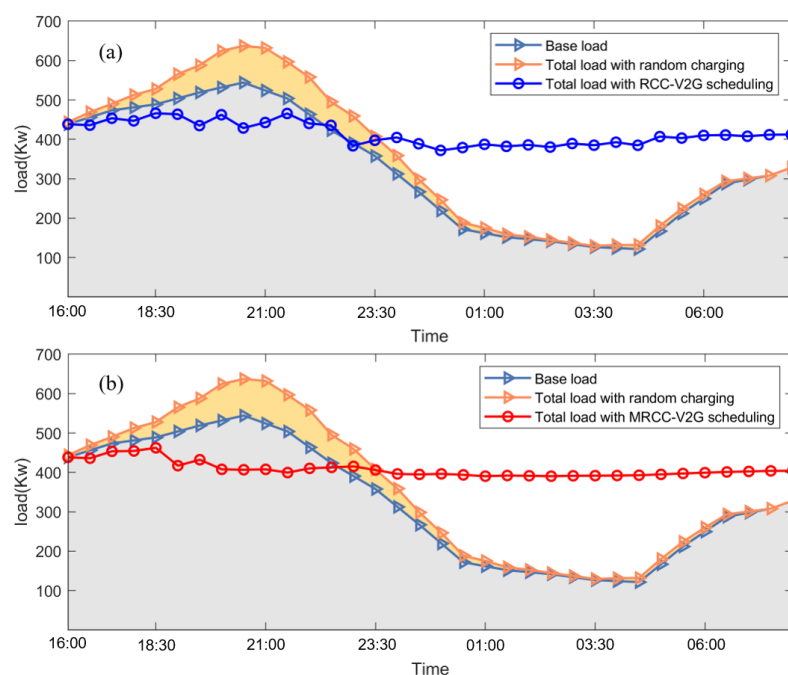


Figure 7. Power system load profile (a) PSO-RCC algorithm and (b) PSO-MRCC method.

5. Conclusions

This paper presents an online V2G scheduling method to mitigate battery aging in V2G services. The approach involves collecting and integrating real-time vehicle information using an online sliding window approach and quantifying battery aging during the scheduling process using the proposed MRCC algorithm. Compared with G-PSO-RCC, this method showed a 1.58% increase in peak load and a 0.78% increase in EFCC, while reducing the STD by 3.8%. It not only achieves results similar to G-PSO-RCC but also meets the requirements of practical scheduling scenarios. Compared to conventional V2G scheduling methods, this approach achieves results closely approximating global optimization, exhibiting an 8.4% reduction in equivalent full-cycle counts and a 28.57% reduction in STD. Further, the modeling approach demonstrates similar improvements when integrated with other intelligent optimization algorithms.

In this paper, we focus on battery aging when users participate in V2G. It is assumed that battery aging is only related to the number of cycles. However, the ambient temperature also has a relatively large impact on battery aging, and higher or lower temperatures will exacerbate battery aging. If EV charging and discharging can be reasonably planned with the battery temperature in V2G scheduling it will avoid the battery working under extreme temperatures and make the system more perfect. Future work could explore the effects of temperature on battery aging and suppress these effects in V2G scheduling.

Author Contributions: Q.Z.: Conceived and designed the experiments; Performed the experiments; Contributed reagents, materials, analysis tools or data; Analyzed and interpreted the data; Wrote the paper. M.I.: Analyzed and interpreted the data; Contributed reagents, materials, analysis tools or data; Wrote the paper. K.X.: Conceived and designed the experiments; Contributed reagents, materials, analysis tools or data; Wrote the paper. All authors have read and agreed to the published version of the manuscript.

Funding: This work is partially supported by the National Natural Science Foundation of China (Grant No. 62073311), the Key Program of Natural Science Foundation of Shenzhen (Grant No. JCYJ20200109115403807), and the Sustainable Development Science and Technology Fund of Shenzhen (Grant No. KCXST20221021111210023).

Data Availability Statement: Data is contained within the article.

Conflicts of Interest: The authors declare no conflicts of interest.

References

1. Chen, Y.; Zhao, C.; Low, S.H.; Wierman, A. An energy sharing mechanism considering network constraints and market power limitation. *IEEE Trans. Smart Grid* **2022**, *14*, 1027–1041. [\[CrossRef\]](#)
2. Kempton, W.; Tomić, J. Vehicle-to-grid power fundamentals: Calculating capacity and net revenue. *J. Power Sources* **2005**, *144*, 268–279. [\[CrossRef\]](#)
3. Das, H.S.; Rahman, M.M.; Li, S.; Tan, C. Electric vehicles standards, charging infrastructure, and impact on grid integration: A technological review. *Renew. Sustain. Energy Rev.* **2020**, *120*, 109618. [\[CrossRef\]](#)
4. Upputuri, R.P.; Subudhi, B. A Comprehensive Review and Performance Evaluation of Bidirectional Charger Topologies for V2G/G2V Operations in EV Applications. *IEEE Trans. Transp. Electrification* **2023**, *10*, 583–595. [\[CrossRef\]](#)
5. Hao, X.; Chen, Y.; Wang, H.; Wang, H.; Meng, Y.; Gu, Q. A V2G-oriented reinforcement learning framework and empirical study for heterogeneous electric vehicle charging management. *Sustain. Cities Soc.* **2023**, *89*, 104345. [\[CrossRef\]](#)
6. Dong, J.; Yassine, A.; Armitage, A.; Hossain, M.S. Multi-Agent Reinforcement Learning for Intelligent V2G Integration in Future Transportation Systems. *IEEE Trans. Intell. Transp. Syst.* **2023**, *24*, 5974–15983. [\[CrossRef\]](#)
7. Rabiee, A.; Sadeghi, M.; Aghaei, J.; Heidari, A. Optimal operation of microgrids through simultaneous scheduling of electrical vehicles and responsive loads considering wind and PV units uncertainties. *Renew. Sustain. Energy Rev.* **2016**, *57*, 721–739. [\[CrossRef\]](#)
8. Sassi, O.; Oulamara, A. Electric vehicle scheduling and optimal charging problem: Complexity, exact and heuristic approaches. *Int. J. Prod. Res.* **2017**, *55*, 519–535. [\[CrossRef\]](#)
9. McCabe, D.; Ban, X.J. Optimal locations and sizes of layover charging stations for electric buses. *Transp. Res. Part C Emerg. Technol.* **2023**, *152*, 104157. [\[CrossRef\]](#)
10. Quintana, C.L.; Arbelaiz, A.; Climent, L. Robust ebus charging location problem. *IEEE Open J. Intell. Transp. Syst.* **2022**, *3*, 856–871. [\[CrossRef\]](#)

11. Kchaou-Boujelben, M. Charging station location problem: A comprehensive review on models and solution approaches. *Transp. Res. Part C Emerg. Technol.* **2021**, *132*, 103376. [[CrossRef](#)]
12. Schneider, M.; Stenger, A.; Goeke, D. The electric vehicle-routing problem with time windows and recharging stations. *Transp. Sci.* **2014**, *48*, 500–520. [[CrossRef](#)]
13. Jin, L.; Zhang, C.K.; He, Y.; Jiang, L.; Wu, M. Delay-dependent stability analysis of multi-area load frequency control with enhanced accuracy and computation efficiency. *IEEE Trans. Power Syst.* **2019**, *34*, 3687–3696. [[CrossRef](#)]
14. Kavousi-Fard, A.; Abunasri, A.; Zare, A.; Hoseinzadeh, R. Impact of plug-in hybrid electric vehicles charging demand on the optimal energy management of renewable micro-grids. *Energy* **2014**, *78*, 904–915. [[CrossRef](#)]
15. Fernandes, C.; Frías, P.; Latorre, J.M. Impact of vehicle-to-grid on power system operation costs: The Spanish case study. *Appl. Energy* **2012**, *96*, 194–202. [[CrossRef](#)]
16. Noel, L.; de Rubens, G.Z.; Kester, J.; Sovacool, B.K. Beyond emissions and economics: Rethinking the co-benefits of electric vehicles (EVs) and vehicle-to-grid (V2G). *Transp. Policy* **2018**, *71*, 130–137. [[CrossRef](#)]
17. Zhou, C.; Qian, K.; Allan, M.; Zhou, W. Modeling of the cost of EV battery wear due to V2G application in power systems. *IEEE Trans. Energy Convers.* **2011**, *26*, 1041–1050. [[CrossRef](#)]
18. Peterson, S.B.; Apt, J.; Whitacre, J. Lithium-ion battery cell degradation resulting from realistic vehicle and vehicle-to-grid utilization. *J. Power Sources* **2010**, *195*, 2385–2392. [[CrossRef](#)]
19. Dubarry, M.; Devie, A.; McKenzie, K. Durability and reliability of electric vehicle batteries under electric utility grid operations: Bidirectional charging impact analysis. *J. Power Sources* **2017**, *358*, 39–49. [[CrossRef](#)]
20. Thingvad, A.; Marinelli, M. Influence of v2g frequency services and driving on electric vehicles battery degradation in the nordic countries. In Proceedings of the Event 31st International Electric Vehicles Symposium & Exhibition & International Electric Vehicle Technology Conference 2018, Kobe, Japan, 30 September–3 October 2018.
21. Calearo, L.; Marinelli, M. Profitability of frequency regulation by electric vehicles in Denmark and Japan considering battery degradation costs. *World Electr. Veh. J.* **2020**, *11*, 48. [[CrossRef](#)]
22. Shao, J.; Li, J.; Yuan, W.; Dai, C.; Wang, Z.; Zhao, M.; Pecht, M. A novel method of discharge capacity prediction based on simplified electrochemical model-aging mechanism for lithium-ion batteries. *J. Energy Storage* **2023**, *61*, 106788. [[CrossRef](#)]
23. Bensaad, Y.; Friedrichs, F.; Baumhöfer, T.; Eswein, M.; Bähr, J.; Fill, A.; Birke, K.P. Embedded real-time fractional-order equivalent circuit model for internal resistance estimation of lithium-ion cells. *J. Energy Storage* **2023**, *67*, 107516. [[CrossRef](#)]
24. Grimaldi, A.; Minuto, F.D.; Perol, A.; Casagrande, S.; Lanzini, A. Ageing and energy performance analysis of a utility-scale lithium-ion battery for power grid applications through a data-driven empirical modelling approach. *J. Energy Storage* **2023**, *65*, 107232. [[CrossRef](#)]
25. Shi, R.; Li, S.; Zhang, P.; Lee, K.Y. Integration of renewable energy sources and electric vehicles in V2G network with adjustable robust optimization. *Renew. Energy* **2020**, *153*, 1067–1080. [[CrossRef](#)]
26. Li, S.; Li, J.; Su, C.; Yang, Q. Optimization of bi-directional V2G behavior with active battery anti-aging scheduling. *IEEE Access* **2020**, *8*, 11186–11196. [[CrossRef](#)]
27. Goebel, C.; Callaway, D.S. Using ICT-controlled plug-in electric vehicles to supply grid regulation in California at different renewable integration levels. *IEEE Trans. Smart Grid* **2012**, *4*, 729–740. [[CrossRef](#)]
28. Bagherinezhad, A.; Alizadeh, M.; Parvania, M. Rolling Horizon Approach for Real-time Charging and Routing of Autonomous Electric Vehicles. *IEEE Open Access J. Power Energy* **2024**, *11*, 94–103. [[CrossRef](#)]
29. Chand, S.; Hsu, V.N.; Sethi, S. Forecast, solution, and rolling horizons in operations management problems: A classified bibliography. *Manuf. Serv. Oper. Manag.* **2002**, *4*, 25–43. [[CrossRef](#)]
30. Jarvis, P.; Climent, L.; Arbelaez, A. Smart and sustainable scheduling of charging events for electric buses. In *EU Cohesion Policy Implementation—Evaluation Challenges Opportunities*; Springer: Berlin/Heidelberg, Germany, 2023; pp. 121–129.
31. Ma, X.; Guo, Y.; Wang, L.; Ji, W. Exploration of the reliability of automotive electronic power steering system using device junction electrothermal profile cycle. *IEEE Access* **2016**, *4*, 7054–7062. [[CrossRef](#)]
32. Liao, Y.T.; Lu, C.N. Dispatch of EV charging station energy resources for sustainable mobility. *IEEE Trans. Transp. Electrif.* **2015**, *1*, 86–93. [[CrossRef](#)]
33. Ruder, S. An overview of gradient descent optimization algorithms. *arXiv* **2016**, arXiv:1609.04747.
34. McGuckin, N.; Fucci, A. *Summary of Travel Trends: 2017 National Household Travel Survey*; Technical Report; Department of Transportation, Federal Highway Administration: Washington, DC, USA, 2018.
35. Liu, J.; Lu, L.; Gao, H.; Liu, J.; Shi, W.; Wu, Y. Planning of active distribution network considering characteristics of distributed generator and electric vehicle. *Autom. Electr. Power Syst.* **2020**, *44*, 41–48.

Disclaimer/Publisher’s Note: The statements, opinions and data contained in all publications are solely those of the individual author(s) and contributor(s) and not of MDPI and/or the editor(s). MDPI and/or the editor(s) disclaim responsibility for any injury to people or property resulting from any ideas, methods, instructions or products referred to in the content.